Distributed Multipolar Expansion Approach to Calculation of Excitation Energy Transfer Couplings

Bartosz Błasiak,*,[†,‡] Michał Maj,[†,‡] Minhaeng Cho,[†,‡] and Robert W. Góra*,[§]

[†]Center for Molecular Spectroscopy and Dynamics, Institute for Basic Science (IBS), Seoul 136-701, Republic of Korea

[‡]Department of Chemistry, Korea University, Seoul 136-701, Republic of Korea

[§]Department of Physical and Quantum Chemistry, Faculty of Chemistry, Wrocław University of Technology, Wybrzeże Wyspiańskiego 27, Wrocław 50-370, Poland

S *Supporting Information*

ABSTRACT: We propose a new approach for estimating the electrostatic part of the excitation energy transfer (EET) coupling between electronically excited chromophores based on the transition density-derived cumulative atomic multipole moments (TrCAMM). In this approach, the transition potential of a chromophore is expressed in terms of truncated distributed multipolar expansion and analytical formulas for the TrCAMMs are derived. The accuracy and computational feasibility of the proposed approach is tested against the exact Coulombic couplings, and various multipole expansion truncation schemes are analyzed. The results of preliminary calculations show that the TrCAMM approach is capable of reproducing the exact Coulombic EET couplings accurately and efficiently and is superior to other widely used schemes: the transition charges from electrostatic potential (TrESP) and the transition density cube (TDC) method.
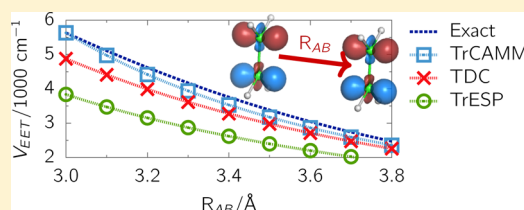
1. INTRODUCTION

At the heart of light harvesting phenomena that occur in all known photosynthetic systems[1−3] is the photophysical process of excitation energy transfer (EET) among chromophores.[2,4] All known photosynthetic systems share a common structure in which the reaction center is surrounded by a network of antenna systems formed by pigment molecules weakly bound to polypeptide chains.[1] Exciton migration is also responsible for performance of organic light-emitting diodes and photovoltaic devices.[5−8] Photodynamic therapy of cancer is yet another promising application of triplet EET.[9]

A key parameter which promotes EET is the electronic coupling of weakly interacting donor and acceptor molecules. It is well-known that the major component of such a coupling is primarily governed by the Coulombic interactions of their transition densities.[10] Despite the fact that the latter can be nowadays quite routinely obtained from electronic structure calculations, evaluation of the exact Coulombic couplings is still often not feasible or is impractical for large molecular systems. Therefore, several approximate theoretical approaches were proposed so far.[10−21]

One of the simplest possible schemes is the so-called point−dipole approximation (PDA) in which the electronic coupling is approximated by interaction of the transition dipole moments representing the transition densities. It was proposed in the seminal work by Förster[11] and nowadays is still being widely used to estimate EET couplings in a variety of biological systems such as the Fenna−Matthews−Olson (FMO) complex of green sulfur bacteria,[22] the LHC-II complex of plants, the PE545 photosystem of marine algae,[23] covalently linked multiporphyrins,[24] and many others. Unfortunately, this scheme does not provide reliable results at short interchromophore distances or, more precisely, when the sizes of the chromophores become comparable to their intermolecular separation.[13,15,25−28] It is, thus, difficult to assign a single threshold value on the latter, but the results of test calculations for common chromophores and fluorescent probes indicate that the PDA estimates start to deviate significantly from the reference values at intermolecular distances smaller than about 12−20 Å.[13,15,25,28] This is mainly due to neglect of higher multipolar contributions and also because the ambiguity in defining the origins of the transition dipoles becomes more pronounced when the monomers are getting closer.

To overcome the limitations of PDA, distributed charge models, which describe the transition charge densities more realistically, were developed. The first approach going beyond the PDA was proposed by Gołębiewski and Witkowski.[12] In their seminal work the transition moments of π-conjugated molecules were represented by the effective atomic π-electronic charges. Later on, the generalized transition monopoles model was often used to quantify electronic excitation interactions between chromophores.[13,14] Currently, among the most frequently used approaches[10,15,16,25−27,29−35] are the transition density cubes (TDC) of Krueger et al.[15] and the transition charges from electrostatic potential (TrESP) proposed by Madjet et al.[16] The treatments in question utilize appropriate discretization of the transition densities, either into the regular cubic grid of point charges (a transition density cube in TDC method) or the sets of atomic transition charges, fitted to the

electrostatic potential (ESP) of the transition charge density (TrESP method). The TDC scheme should provide, in principle, nearly exact estimations of the Coulombic EET coupling, provided that one uses sufficiently large and dense TDCs. However, noticeable deteriorations of the results were reported when the TDCs of interacting species strongly overlap.[18] In such a case, the distance between the two interacting cube elements may become close to zero and the method encounters singularity. This can be amended by imposing appropriate cutoff distances, but such a procedure must affect the accuracy. More importantly, the estimated couplings depend significantly on the density and dimensions of the grid.[26,34] Particularly, the finite size of density cubes results in underestimation of the charge-penetration effects due to exponential decay and diffuse character of the transition charge densities. The TDC method is also quite demanding computationally and becomes impractical for large chromophores because the number of grid points can easily exceed hundreds of thousands. This difficulty is amended in the TrESP scheme where the number of distributed sites is equal to the number of atoms. However, this inevitably leads to a loss of accuracy, which is particularly pronounced at smaller interchromophore distances. Indeed, it is still unclear to what extent the TrESP method reproduces the exact electrostatic EET couplings at small intermolecular separations.[32,34] In particular, it was shown that the TrESP method can substantially underestimate the couplings,[21] and the values obtained by using TDC and TrESP schemes can differ substantially.[34] For this reason, retaining a relatively small number of mapping centers while preserving an accurate description of the transition density distribution at the same time still poses difficulty.

Recently, an extension of TrESP protocol was proposed by Fujimoto in which the atomic transition charges (C) are augmented with the atomic dipoles (D) and quadrupoles (Q) derived from electrostatic potential fitting (TrESP-CDQ).[21] The TrESP-CDQ approach proposed by Fujimoto shows major improvement with respect to the original TrESP method. However, it relies on arbitrary selection of a grid to fit the transition multipoles and the particulars of the fitting procedure itself. In order to ensure a unique and more general solution, independent of the fitting procedure, in this work we propose a new scheme based on the distributed multipolar expansion which provides almost exact values of the Coulombic part of EET couplings while requiring negligible computational effort. Our scheme, conceptually similar to those discussed previously, is based on the distributed multipolar expansion of the one-particle transition densities obtained from *ab initio* or the time-dependent density functional theory (TD-DFT) calculations. For this end, we use the cumulative atomic multipole moments scheme (CAMM)[36] up to hexadecapoles, and hence, we shall use the TrCAMM acronym to describe our procedure. In the following section we outline the details of the TrCAMM protocol along with a brief description of other approximate schemes that were proposed thus far. Next, the TrCAMM results obtained for the chosen model systems (ethylene, naphthalene, and 7-aminocoumarin homomolecular dimers) are discussed and compared to those estimated using the TDC and TrESP schemes as well as the results of direct calculations of the Coulombic interactions between transition densities.

2. COMPUTATIONAL METHODS

The theory of electronic EET couplings was recently thoroughly reviewed;[4,19,20,37] thus, in this section we give only a brief overview of the methodology relevant for the approach that we propose. For this purpose it is sufficient to focus on the couplings between two interacting molecules A and B which can be either in ground (g) or excited state (e). Within Born−Oppenheimer approximation the electronic Hamiltonian of such an aggregate can be partitioned into intra- and intermolecular contributions:

$$\mathcal{H}_{AB} = \mathcal{H}_A + \mathcal{H}_B + \mathcal{V}_{AB} \tag{1}$$

where $\mathcal{H}_A$ and $\mathcal{H}_B$ are the Hamiltonians of isolated molecules and $\mathcal{V}_{AB}$ represents the intermolecular interaction potential between electrons and nuclei of interacting species. If the latter is small, the dimer Hamiltonian can be expanded in terms of the adiabatic electronic states of noninteracting species (φ). Consequently, the dimer wave function $|\psi\rangle$ can be expanded in terms of antisymmetrized Hartree products of these states (ϕ):

$$\psi(\mathbf{r}; \mathbf{R}) = \sum_i c_i \phi_i \tag{2}$$

where

$$\phi_i = \mathcal{A} \varphi_{a_i}(\mathbf{r}_A; \mathbf{R}_A) \, \varphi_{b_i}(\mathbf{r}_B; \mathbf{R}_B) \tag{3}$$

$\mathbf{r}$ and $\mathbf{R}$ are the sets of electronic and nuclear coordinates of the aggregate, respectively, whereas $\mathbf{r}_M$ and $\mathbf{R}_M$ are the corresponding coordinates of monomer M.

Perturbation theory through the first order yields the following expression for the electronic part of V_{AB} matrix element:[37]

$$\langle \phi_i | \mathcal{V}_{AB} | \phi_j \rangle = \int d\mathbf{r}_A \, d\mathbf{r}_B \, \mathcal{A}[\varphi_{a_i}^*(\mathbf{r}_A; \mathbf{R}) \, \varphi_{b_i}^*(\mathbf{r}_B; \mathbf{R})]$$
$$\times \mathcal{V}_{AB} \mathcal{A}[\varphi_{b_j}(\mathbf{r}_B; \mathbf{R}) \, \varphi_{a_j}(\mathbf{r}_A; \mathbf{R})]$$
$$\equiv J_{AB}(a_i b_i, b_j a_j) - K_{AB}(a_i b_i, b_j a_j) \tag{4}$$

The matrix elements relevant for EET couplings in the considered approximation are $J_{AB}(eg,eg)$ and $K_{AB}(eg,eg)$. Introducing a one-particle transition density matrix of molecule M, corresponding to a transition between ground g and excited state e,

$$\rho_M^{eg}(\mathbf{x}_1; \mathbf{x}_1')$$
$$= N_M \int d\mathbf{x}_2 \, ... \, d\mathbf{x}_{N_M} \, \varphi_e(\mathbf{x}_1, ..., \mathbf{x}_{N_M}) \, \varphi_g^*(\mathbf{x}_1', ..., \mathbf{x}_{N_M}) \tag{5}$$

where $\mathbf{x}_i \equiv (\mathbf{r}_i, s_i)$ and then integrating over the spin coordinates:

$$\rho_M^{eg}(\mathbf{r}_1; \mathbf{r}_1') = \int ds_1 \int ds_1' \, \rho_M^{eg}(\mathbf{x}_1; \mathbf{x}_1') \tag{6}$$

the Coulombic and exchange contributions to the off-diagonal matrix element V_{AB} can be put as follows:

$$V_{AB} = \int d\mathbf{r}_1 \, d\mathbf{r}_1' \, \frac{\rho_A^{eg*}(\mathbf{r}_1; \mathbf{r}_1) \, \rho_B^{eg}(\mathbf{r}_1'; \mathbf{r}_1')}{|\mathbf{r}_1 - \mathbf{r}_1'|}$$
$$- \frac{1}{2} \int d\mathbf{r}_1 \, d\mathbf{r}_1' \, \frac{\rho_A^{eg*}(\mathbf{r}_1; \mathbf{r}_1') \, \rho_B^{eg}(\mathbf{r}_1'; \mathbf{r}_1)}{|\mathbf{r}_1 - \mathbf{r}_1'|}$$
$$\equiv J_{AB}(eg, eg) - K_{AB}(eg, eg) \tag{7}$$

$J_{AB}(eg,eg)$ in the preceding expression is central to the present study, as it represents the Coulombic part of the excitonic coupling, being the major contribution at large and intermediate intermolecular separations. $K_{AB}(eg,eg)$ is the corresponding exchange–repulsion contribution.

2.1. TrCAMM Method. In general, the difficulty in evaluating the integral in $J_{AB}(eg,eg)$ from eq 7 can be overcome by introducing a distributed-multipole expansion of a transition potential due to molecule M,

$$v_M^{eg}(\mathbf{r}) = \int d\mathbf{r}_1{'} \frac{\rho_M^{eg}(\mathbf{r}_1{'}; \mathbf{r}_1{'})}{|\mathbf{r} - \mathbf{r}_1{'}|}$$
$$= \sum_{k \in M}^{n_M} \left[\mathbf{T}^{(0)} q_k^{eg} - \mathbf{T}^{(1)} \cdot \boldsymbol{\mu}_k^{eg} + \frac{1}{3} \mathbf{T}^{(2)} : \Theta_k^{eg} - \ldots \right]$$
(8)

which leads to[38,39]

$$J_{AB}(eg, eg)$$
$$\cong \sum_{k \in A}^{n_A} \left[q_k^{eg} v_B^{eg}(\mathbf{r}_k) + \boldsymbol{\mu}_k^{eg} \cdot \nabla v_B^{eg}(\mathbf{r}_k) + \frac{1}{3}\Theta_k^{eg} : \nabla \otimes \nabla v_B^{eg}(\mathbf{r}_k) + \ldots \right]$$
(9)

In eq 8 we introduced the *distributed transition charge, dipole, and quadrupole moments* (q_k^{eg}, $\boldsymbol{\mu}_k^{eg}$, and Θ_k^{eg}) representing a part of the transition density distribution of molecule M, whereas the tensors $\mathbf{T}^{(R)}$ are the conventional Rth rank Cartesian "interaction tensors" which can be found elsewhere.[39] In eq 8 and eq 9 multipole moments of rank 2 and higher are assumed to be traceless properties.[38,39]

The distributed multipoles from eq 8 can be obtained by dividing the total (molecular) multipole moments into parts in such a way that the sum of all distributed moments will accumulate to the total quantities. In the case of EET coupling constant, all of the nuclear charge contributions to the total transition multipole moments will vanish due to the orthogonality of adiabatic states.[37] Therefore, one needs to consider only the electronic operator of the multipole moment and neglect the nuclear charges. Namely,

$$\mathcal{M}_{klm}^{el}(\mathbf{r}_0) = -\sum_i (x_i - x_0)^k (y_i - y_0)^l (z_i - z_0)^m$$
(10)

which is defined with respect to the origin at $\mathbf{r}_0$. In eq 10 the summation is performed over all electrons in the monomer. Note that the rank of such a multipole operator is $k + l + m$, so, for example, the dipole moment has three components corresponding to (k,l,m) values equal to $(1,0,0)$, $(0,1,0)$, and $(0,0,1)$, respectively. We emphasize also that the operator in eq 10 defines quadrupole and higher moments in primitive forms. However, their conversion to the corresponding traceless moments that are needed in eqs 8 and 9 is straightforward.[38,39]

Now, in the atomic orbital (AO) basis, the primitive transition multipole moment is

$$M_{klm}^{eg}(\mathbf{r}_0) = \sum_{rs} P_{rs}^{M,eg} \langle r | \mathcal{M}_{klm}^{el}(\mathbf{r}_0) | s \rangle$$
(11)

where $P_{rs}^{M,eg}$ is the transition density matrix element of molecule M and $|r\rangle$, $|s\rangle$ are the basis functions (AOs). Following Sokalski and Poirier,[36] we look for such a division of $M_{klm}^{eg}(\mathbf{r}_0)$ among all atomic sites, such that

$$M_{klm}^{eg}(\mathbf{r}_0) = \sum_I M_{I,klm}^{eg}(\mathbf{r}_0)$$
$$= \sum_I \left(\sum_{r \in I} \sum_{\text{all } s} P_{rs}^{M,eg} \langle r | \mathcal{M}_{klm}^{el}(\mathbf{r}_0) | s \rangle \right)$$
(12)

where index I runs over all atoms in molecule M. However, according to eq 12, M_{klm}^{eg} are all centered at the same point in space which can be far from its corresponding atomic center. Therefore, one needs to recenter them in order to shift the origins to the atomic sites according to the following recurrence relation:[36]

$$M_{I,klm}^{eg,\text{CAMM}} = M_{I,klm}(\mathbf{0}) - \sum_{\substack{k' \geq 0 \\ k'l'm' \neq klm}}^{k} \sum_{l' \geq 0}^{l} \sum_{m' \geq 0}^{m} \binom{k}{k'}\binom{l}{l'}\binom{m}{m'}$$
$$\times x_I^{k-k'} y_I^{l-l'} z_I^{m-m'} M_{I,k'l'm'}^{eg,\text{CAMM}}$$
(13)

Hence, eqs 13 and 12 define the distributed transition cumulative atomic multipole moment $M_{I,klm}^{eg,\text{CAMM}}$, here abbreviated as TrCAMM. The TrCAMM method can then be considered as a modification of the original CAMM formulation because the particular TrCAMMs are exactly the same as in eqs 8–11 from ref 36, apart from the nuclear terms which vanish, and the density matrix element which is replaced by the transition density matrix element. For the sake of completeness, we provide the explicit formulas for the transition cumulative charge, dipole, quadrupole, octupole, and hexadecapole moments, respectively:

$$q_I^{eg} = -\sum_{r \in I} \sum_s P_{rs}^{M,eg} \langle r|s \rangle$$
(14)

$$\mu_I^{eg} = \sum_{r \in I} \sum_s P_{rs}^{M,eg} [\langle r|s \rangle \mathbf{R}_I - \langle r|\mathbf{r}|s \rangle]$$
(15)

$$\Theta_I^{eg} = \sum_{r \in I} \sum_s P_{rs}^{M,eg} [-\mathbf{R}_I \otimes \mathbf{R}_I \langle r|s \rangle + \mathbf{R}_I \otimes \langle r|\mathbf{r}|s \rangle$$
$$+ \langle r|\mathbf{r}|s \rangle \otimes \mathbf{R}_I - \langle r|\mathbf{r} \otimes \mathbf{r}|s \rangle]$$
(16)

$$\Omega_I^{eg} = \sum_{r \in I} \sum_s P_{rs}^{M,eg} [\mathbf{R}_I \otimes \mathbf{R}_I \otimes \mathbf{R}_I \langle r|s \rangle - \mathbf{R}_I \otimes \mathbf{R}_I \otimes \langle r|\mathbf{r}|s \rangle$$
$$- \mathbf{R}_I \otimes \langle r|\mathbf{r}|s \rangle \otimes \mathbf{R}_I - \langle r|\mathbf{r}|s \rangle \otimes \mathbf{R}_I \otimes \mathbf{R}_I$$
$$+ \mathbf{R}_I \otimes \langle r|\mathbf{r} \otimes \mathbf{r}|s \rangle + \langle r|\mathbf{r} \otimes \mathbf{R}_I \otimes \mathbf{r}|s \rangle$$
$$+ \langle r|\mathbf{r} \otimes \mathbf{r}|s \rangle \otimes \mathbf{R}_I - \langle r|\mathbf{r} \otimes \mathbf{r} \otimes \mathbf{r}|s \rangle]$$
(17)

$$\Xi_I^{eg} = \sum_{r \in I} \sum_s P_{rs}^{M,eg} [-\mathbf{R}_I \otimes \mathbf{R}_I \otimes \mathbf{R}_I \otimes \mathbf{R}_I \langle r|s \rangle$$
$$+ \mathbf{R}_I \otimes \mathbf{R}_I \otimes \mathbf{R}_I \otimes \langle r|\mathbf{r}|s \rangle + \mathbf{R}_I \otimes \mathbf{R}_I \otimes \langle r|\mathbf{r}|s \rangle \otimes \mathbf{R}_I$$
$$+ \mathbf{R}_I \otimes \langle r|\mathbf{r}|s \rangle \otimes \mathbf{R}_I \otimes \mathbf{R}_I + \langle r|\mathbf{r}|s \rangle \otimes \mathbf{R}_I \otimes \mathbf{R}_I \otimes \mathbf{R}_I$$
$$- \mathbf{R}_I \otimes \mathbf{R}_I \otimes \langle r|\mathbf{r} \otimes \mathbf{r}|s \rangle - \mathbf{R}_I \otimes \langle r|\mathbf{r} \otimes \mathbf{r}|s \rangle \otimes \mathbf{R}_I$$
$$- \langle r|\mathbf{r} \otimes \mathbf{r}|s \rangle \otimes \mathbf{R}_I \otimes \mathbf{R}_I + \mathbf{R}_I \otimes \langle r|\mathbf{r} \otimes \mathbf{r} \otimes \mathbf{r}|s \rangle$$
$$+ \langle r|\mathbf{r} \otimes \mathbf{r} \otimes \mathbf{r}|s \rangle \otimes \mathbf{R}_I - \mathbf{R}_I \otimes \langle r|\mathbf{r} \otimes \mathbf{R}_I \otimes \mathbf{r}|s \rangle$$
$$- \langle r|\mathbf{r} \otimes \mathbf{R}_I \otimes \mathbf{r}|s \rangle \otimes \mathbf{R}_I - \langle r|\mathbf{r} \otimes \mathbf{r} \otimes \mathbf{r}|s \rangle$$
$$+ \langle r|\mathbf{r} \otimes \mathbf{R}_I \otimes \mathbf{r}|s \rangle + \langle r|\mathbf{r} \otimes \mathbf{R}_I \otimes \mathbf{r}|s \rangle$$
$$- \langle r|\mathbf{r} \otimes \mathbf{R}_I \otimes \mathbf{R}_I \otimes \mathbf{r}|s \rangle]$$
(18)

In the preceding equations, $\mathbf{R}_I$ denotes the position vector of the Ith nucleus and $\otimes$ is an outer tensor product.
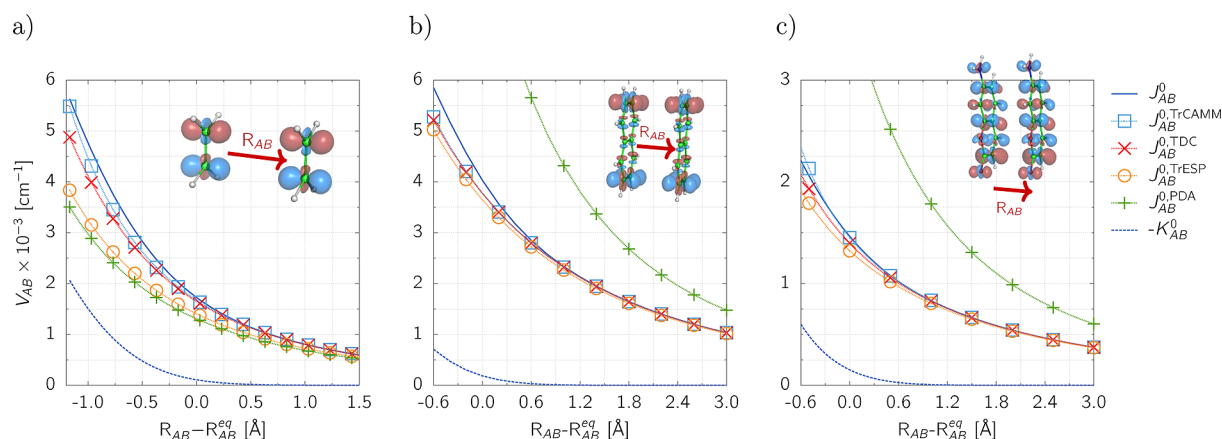
Figure 1. Excitonic couplings of ethylene (a), naphthalene (b), and 7-aminocoumarin (c) dimers in stacking alignment estimated using selected approximate electrostatic models for varying intermolecular separation R_{AB}.

It should be noted that there are also other schemes which could be used to partition the multipole moments.[40,41] However, here we chose the orbital-space-based scheme because of its simplicity.

2.2. Relationships with Other Approaches. It is instructive to consider the previous approaches with respect to certain limiting cases of the distributed transition multipoles introduced in this work. In the limit where we constrain the distributions in eq 8 to keep only a single center on each chromophore (i.e., $n_M = 1$ for $M = A,B$) the transition charges will add up to zero due to the orthogonality of ground and excited state wave functions of the monomers. If we also truncate the multipole expansions on the dipolar terms, we will arrive at the PDA:

$$J_{AB}(eg, eg) \approx \frac{\boldsymbol{\mu}_A^{eg} \cdot \boldsymbol{\mu}_B^{eg} - 3(\boldsymbol{\mu}_A^{eg} \cdot \mathbf{e}_R)(\boldsymbol{\mu}_B^{eg} \cdot \mathbf{e}_R)}{R_{AB}^3} \quad (19)$$

which, in this case, is the leading term in the expansion from eq 9. In eq 19 A and B denote the origins of transition dipoles of interacting species, separated by a distance R_{AB}.

If we use a very large number of distributed points, the contributions to the transition potentials from distributed dipoles and higher multipoles will vanish and only the distributed charges will contribute. Moreover, if we choose the distributed charges to be placed in a regular cubic grid of points, surrounding the molecule in question, we reach essentially the TDC approximation; i.e.,

$$J_{AB}(eg, eg) \cong \sum_{k \in A}^{n_A} \sum_{l \in B}^{n_B} \frac{q_k^{eg} q_l^{eg}}{r_{kl}} \quad (20)$$

where the transition charges are determined on a rectangular grid of points with spacings δx, δy, and δz as follows:

$$q_{k \in M}^{eg}(x, y, z)$$
$$= \delta x \, \delta y \, \delta z \int_x^{\delta x} \int_y^{\delta y} \int_z^{\delta z} \int_s \mathrm{d}s \, \mathrm{d}x \, \mathrm{d}y \, \mathrm{d}z \, \varphi_e \, \varphi_g^* \quad (21)$$

Transition charges and higher multipoles can also be obtained from fitting to the exact transition potential, given in the integral formula in eq 8, which leads to the TrESP and TrESP-CDQ schemes, respectively. In such a case one can follow the same procedure as in the conventional ESP technique[16] or use some modifications such as in the ChelpBOW method of

Sigfridsson and Ryde.[42] However, it becomes clear that the TrCAMM method introduced earlier, which is based on the generalized distributed-multipole approach and does not rely on any adjustable parameters (such as the dimensions and density of grids used to calculate the electrostatic potential in the TrESP and TrESP-CDQ methods or the distributed charges in TDC approach), is the most versatile among all of the approximate methods.

2.3. Computational Details. In order to demonstrate the performance of the TrCAMM scheme, we have chosen dimers of ethylene, naphthalene, and 7-aminocoumarin as model systems. The equilibrium geometries for the stacking alignment of the molecules were optimized at the MP2/6-31G(d) level assuming D_{2h} (for ethylene and naphthalene dimers) or C_s (for 7-aminocoumarin dimer) point group symmetries of the complexes, and subsequently the transition densities between the ground and the excited states for each monomer were calculated using the CIS/6-31G(d) approach, as implemented in the Gaussian 09 package.[43]

The corresponding one-particle transition density matrices were then used to generate the transition cumulative atomic multipole moments (TrCAMMs) up to hexadecapoles, the fitted transition charges (TrESPs), and the transition density cubes (TDCs). The TrESP scheme was implemented according to the procedure described by Fujimoto.[18] Here, randomly chosen sets of 3000 points per atom were used to fit the charges from the transition density ESP, given in the integral form in eq 8. The transition density cubes were generated on a rectangular grid extending 6 au in each direction from the terminal atoms and assuming a uniform spacing of 0.2 au (δx, δy, and δz in eq 21) in all directions. The accuracy of the obtained cube files was tested against those produced by the Q-Chem package[44] at the same level of theoretical approximation. The corresponding coupling constants were calculated using the sixth version of the Coupling package of Krueger et al.[15] The results obtained using the TrCAMM, TrESP, and TDC schemes are compared with the exact Coulombic couplings J_{AB} (cf. eq 7) calculated using either our custom code interfaced with the Libint library[45] or the matrop routine available in the MOLPRO package.[46] In some cases the corresponding exchange−repulsion contribution K_{AB} is also reported to indicate the extent of overlap of the transition charge densities. The same one-particle transition density matrices were used to derive the parameters of the TrCAMM, TrESP, and TDC methods, and to compute the J_{AB} and K_{AB} values.
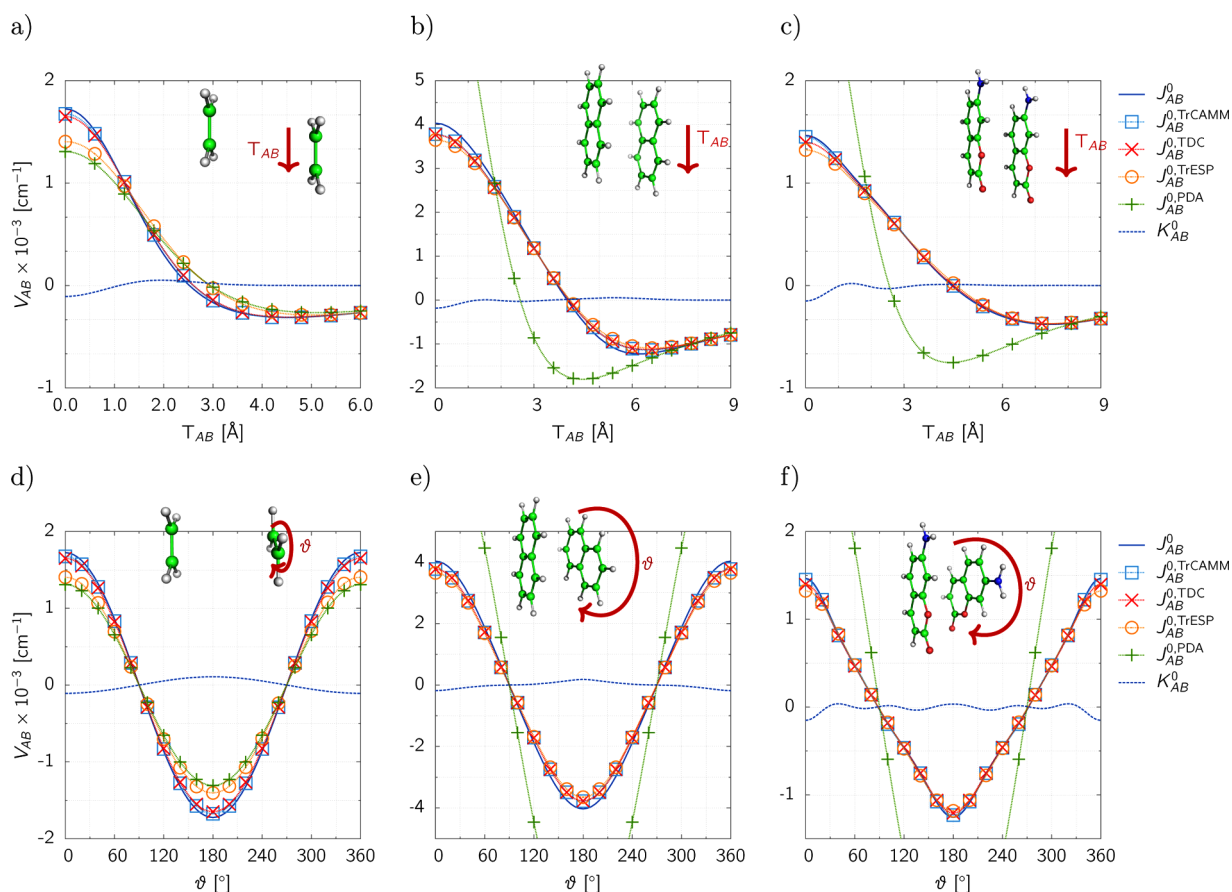
Figure 2. Excitonic couplings of ethylene (a, d), naphthalene (b, e), and 7-aminocoumarin (c, f) dimers in stacking alignment estimated using selected approximate electrostatic models for varying intermolecular orientation: slide (top panels) and rotation (bottom panels).

3. RESULTS AND DISCUSSION

In order to test the performance of the TrCAMM method, we considered ethylene, naphthalene, and 7-aminocoumarin dimers in stacking alignment and calculated the distance- and angle-dependent scans of the electrostatic EET couplings between the bright $\pi\pi^*$ states (1^1B_{1u}, 2^1B_{2u}, and $1^1A'$, respectively) using the CIS method with 6-31G(d) basis set. The CIS method captures the qualitative features of the transition charge density distributions for the chosen states, which is sufficient for comparison of the selected approximate electrostatic schemes. The contour plots of the transition densities are shown as insets in Figure 1. The corresponding transition dipole moments (and oscillator strengths) are $\mu_z = -1.708$ au ($f = 0.613$) for ethylene, $\mu_y = 3.655$ au ($f = 2.398$) for naphthalene, and $\mu_x = 2.300$ au, $\mu_y = -0.235$ au ($f = 0.663$) for 7-aminocoumarin. In the case of ethylene dimer, the type and range of considered geometrical displacements from the local minimum correspond to those analyzed previously by Fujimoto (see also the insets in Figures 1 and 2).[19] Analogous displacements were investigated in the cases of naphthalene and 7-aminocoumarin dimers. The equilibrium separations between the molecular planes (R_{AB}^{eq}) are 4.169, 3.623, and 3.600 Å for ethylene, naphthalene, and 7-aminocoumarin dimers, respectively.

The results shown in Figures 1 and 2 demonstrate that for ethylene dimer our TrCAMM estimates are nearly identical to the exact magnitudes of Coulombic couplings J_{AB}^0 (null in the superscript indicates that these quantities correspond to the unrelaxed densities of isolated monomers). This is particularly

noticeable when distances shorter than equilibrium separation are considered (see Figure 1a). In this region of the potential energy surface the values produced by TDC and TrESP approaches are systematically underestimated. It is interesting to note that the TrESP estimates are in this case quite close to the PDA values and both differ substantially from the exact results even at the equilibrium and slightly larger distances. Similar conclusions can be drawn from analysis of the results obtained for varying slide displacement and rotation about the intermolecular axis (see Figure 2), although in these cases the agreement between the TrCAMM and TDC values is much better. In the case of naphthalene dimer the TrCAMM and TDC schemes produce nearly identical results, but the former at a small fraction of computational effort required to compute interactions between TDCs, which were composed of 796080 point charges. A slightly worse performance of the TDC method is observed for 7-aminocoumarin dimer, as it underestimates the exact Coulombic couplings at separations smaller than equilibrium distances, whereas the TrCAMM results are in quantitative agreement with the reference values. Also the TrESP estimates are much better in the cases of naphthalene and 7-aminocoumarin dimers and only at small intermolecular separations become slightly underestimated. This indicates that for larger molecules, having more fitting centers, the performance of the TrESP protocol should improve, at least for complexes relatively close to the equilibrium geometry. To demonstrate this, we performed test calculations at the CIS/6-31G(d) level for the modified chlorophyll a dimer (Chla$_{611}$−Chla$_{612}$) of the LHC-II from

spinach.[16] In this case the exact Coulombic coupling amounts to 327.7 cm^{-1}, while all of the approximate methods gave essentially identical values (321.6 cm^{-1} for TDC, 319.9 cm^{-1} for TrCAMM, and 315.0 cm^{-1} for TrESP). However, in this case the overlap of the transition densities is rather small ($K_{AB}^0 = -0.4$ cm^{-1}). As expected the PDA model, which was quite reliable in the case of the compact molecular structure of ethylene, fails completely in the vicinity of the van der Waals (vdW) minima for naphthalene and 7-aminocoumarin dimers and becomes reliable only when the distances between the molecular centers of charge become larger than about 8 Å. In general, as the intermolecular separations increase, all of the calculated couplings converge to the same value. It is important to note that, in order to evaluate the TrCAMM couplings, the computational effort is only slightly larger than that with TrESP and several orders of magnitude smaller than that with TDC. For instance, in the case of naphthalene dimer the elapsed time of calculations of the excitonic couplings between the TDCs (composed of nearly 800000 points) was about 120 min and was substantially longer than that required to compute the exact Coulombic coupling (about 3 min). In comparison the time required to compute the TrESP and TrCAMM couplings is negligible as it amounts to less than 0.01 s and about 0.45 s, respectively (see Table S1 in the Supporting Information for more details and timings for other systems).

Since the preceding discussion is based on the results obtained using a rather modest basis set, we now comment on the possible basis set extension effects. In this work we focus on the accuracy of the selected approximations of the first-order electrostatic contribution. Thus, the calculated couplings should not depend significantly on the basis set size. Particularly since we do not investigate the effects of dynamical electron correlation on the calculated one-particle transition densities. The electron correlation effects are expected to be significant but should not affect our conclusions regarding applicability of the investigated approximate electrostatic schemes. The results obtained for ethylene dimer using cc-pVDZ and cc-pVTZ basis sets are shown in Figures S1 and S2 as Supporting Information. Indeed, the effects of basis set extension are rather small (see Supporting Information Figure S1). More importantly, the relative performance of the approximate electrostatic schemes does not change appreciably with basis set size (see Supporting Information Figure S2). Thus, the choice of basis set should not affect the general conclusions regarding the performance of the TrCAMM approach based on the results obtained in the 6-31G(d) basis set.

Another relevant technical issue related to TrCAMM procedure is the effect of truncation of the multipolar expansion of electrostatic interaction. The latter is based on a power series expansion of the inverse of the distance between the centers of charge distribution $|\mathbf{R}|^{-1}$. In principle this series should be divergent, since the integration is performed over all space and the charge distributions extend to infinity. However, in the long-range limit the expansion truncated on the low-order terms shows correct asymptotic behavior.[39] It is well-known that the distributed multipolar expansion improves greatly the convergence of the series,[39] but, nonetheless, the expansion has to be truncated. In practice, one could include all of the possible interactions between available multipoles up to a given rank. This method was used by Fujimoto, who included interaction between all distributed charges, dipoles, and quadrupoles in his TrESP-CDQ approach.[21] However, there is another way of truncating the series that is based on the

asymptotic character of interactions among distributed multipoles. In this approach interactions between multipole moments are included only if the sum of their ranks ($l + l'$) is less than or equal to some limiting value. Since the interaction between multipoles falls off as $|R|^{-(l+l'+1)}$ in the latter approach, all of the terms having the same asymptotic behavior are retained. Such an approach is arguably a better choice for central multipole expansion; however, it is not so obvious for distributed multipolar expansions especially at relatively short distances. A comparison of the TrCAMM estimates obtained using various truncation schemes for ethylene dimer in the vicinity of the vdW minimum is shown in Figure S3 in the Supporting Information. Clearly TrCAMM-R^{-5} appears to be the best choice, showing the most consistent performance for all of the tested basis sets. That is why all of the TrCAMM results shown in Figures 1 and 2 were obtained from the multipolar expansion truncated on $|R|^{-5}$ terms. It is interesting to note that the results of TrCAMM-CDQO, including all interactions between available distributed moments up to octupoles (O), are almost identical to the TrCAMM-R^{-5} values and the TrCAMM-CDQ estimates are also very close. In fact, in the short-range limit and for the less flexible basis sets, the TrCAMM-CDQ estimates are even slightly closer to the reference values of J_{AB}^0, most likely due to fortuitous cancellation of errors.

In practical applications the proposed TrCAMM approach should produce results similar to those of the TrESP-CDQ scheme. However, there are a few advantages of the present approach. First, it does not require any additional parameters (such as the arbitrary selection of a grid to fit the transition multipoles in the TrESP-CDQ). Second it provides a unique solution that is not ensured by the fitting procedure adopted in the latter, especially in the case of larger molecules. Finally, the extension of the TrCAMM approach to higher order multipoles is quite straightforward, and although in principle the same applies also to TrESP-CDQ, fitting of higher order multipoles could be much more problematic.

4. SUMMARY AND OUTLOOK

We introduce an approximate method for estimation of the Coulombic excitation energy transfer couplings that is based on a distributed multipolar expansion of the one-particle transition densities using the cumulative atomic multipole moments (CAMM) scheme of Sokalski and Poirier.[36] Our TrCAMM approach outperforms other widely used approximate electrostatic schemes in terms of accuracy and is computationally very efficient.

The results of our preliminary calculations performed on ethylene, naphthalene, and 7-aminocoumarin homomolecular dimers in stacking alignment show that the predicted Coulombic EET couplings reproduce the reference values with great accuracy and at a fraction of computational costs. Although our test results were obtained using a very simple model wave function, the TrCAMM protocol can be easily applied with virtually any wave function or density functional method, provided that the one-particle transition densities are available.

Nonetheless, we need to emphasize that a number of issues should be addressed in the future. In practical applications, the TrESP and TDC methods were often combined with an empirical scaling procedure taking into account the polarization effects due to the surrounding medium.[15,32,47] Although in

principle such effects could be to some extent included already at the stage of transition density calculations using QM/MM types of approaches or even continuous models of solvent, this aspect requires further studies.

We hope that the TrCAMM approach could be of particular use in theoretical modeling of EET processes, particularly when the distances between involved chromophores are relatively small. We demonstrated that our TrCAMM method provides accurate estimates of EET couplings and it is based on a rigorous theoretical model which does not rely on any empirical parameters or fitting procedure.

■ ASSOCIATED CONTENT

⑤ Supporting Information

Text describing analysis of the basis set extension effects and comparison of various truncation schemes of the distributed multipolar expansion, figures showing Coulombic couplings of ethylene $\pi\pi^*$ states, and tables listing comparison of elapsed times of EET coupling computation and the calculated TrCAMMs for the studied molecules. The Supporting Information is available free of charge on the ACS Publications website at DOI: 10.1021/acs.jctc.5b00216.

■ AUTHOR INFORMATION

Corresponding Authors
*(B.B.) E-mail: blasiak.bartosz@gmail.com.
*(R.W.G.) E-mail: robert.gora@pwr.edu.pl.

Notes
The authors declare no competing financial interest.

■ REFERENCES

(1) Pullerits, T.; Sundström, V. *Acc. Chem. Res.* **1996**, *29*, 381−389.

(2) van Amerongen, H.; Valkunas, L.; van Grondelle, R. *Photosynthetic Excitons*; World Scientific: Singapore, 2000; pp 1−118.

(3) Blankenship, R. E. *Molecular Mechanisms of Photosynthesis*; Blackwell Science: Oxford, U.K., 2002; pp 1−123.

(4) Olaya-Castro, A.; Scholes, G. D. *Int. Rev. Phys. Chem.* **2011**, *30*, 49−77.

(5) Sun, Y.; Giebink, N. C.; Kanno, H.; Ma, B.; Thompson, M. E.; Forrest, S. R. *Nature* **2006**, *440*, 908−912.

(6) Farinola, G. M.; Ragni, R. *Chem. Soc. Rev.* **2011**, *40*, 3467−3482.

(7) Grätzel, M. *J. Photochem. Photobiol., C* **2003**, *4*, 145−153.

(8) Nazeeruddin, M. K.; Baranoff, E.; Grätzel, M. *Sol. Energy* **2011**, *85*, 1172−1178.

(9) Robertson, C. A.; Evans, D. H.; Abrahamse, H. *J. Photochem. Photobiol., B* **2009**, *96*, 1−8.

(10) Renger, T. *Photosynth. Res.* **2009**, *102*, 471−485.

(11) Förster, T. *Ann. Phys.* **1948**, *437*, 55−75.

(12) Golebiewski, A.; Witkowski, A. *Rocz. Chem.* **1959**, *33*, 1443−1453.

(13) Chang, J. C. *J. Chem. Phys.* **1977**, *67*, 3901−3909.

(14) Damjanović, A.; Ritz, T.; Schulten, K. *Phys. Rev. E* **1999**, *59*, 3293−3311.

(15) Krueger, B. P.; Scholes, G. D.; Fleming, G. R. *J. Phys. Chem. B* **1998**, *102*, 5378−5386.

(16) Madjet, M. E.; Abdurahman, A.; Renger, T. *J. Phys. Chem. B* **2006**, *110*, 17268−17281.

(17) Hsu, C.-P.; You, Z.-Q.; Chen, H.-C. *J. Phys. Chem. C* **2008**, *112*, 1204−1212.

(18) Fujimoto, K. J. *J. Chem. Phys.* **2010**, *133*, No. 124101.

(19) Fujimoto, K. J. *J. Chem. Phys.* **2012**, *137*, No. 034101.

(20) You, Z.-Q.; Hsu, C.-P. *Int. J. Quantum Chem.* **2014**, *114*, 102−115.

(21) Fujimoto, K. J. *J. Chem. Phys.* **2014**, *141*, No. 214105.

(22) Cho, M.; Vaswani, H. M.; Brixner, T.; Stenger, J.; Fleming, G. R. *J. Phys. Chem. B* **2005**, *109*, 10542−10556.

(23) Aghtar, M.; Kleinekathöfer, U. *J. Lumin.* **2014**, DOI: 10.1016/j.jlumin.2014.11.001.

(24) Yoon, Z. S.; Yoon, M.-C.; Kim, D. *J. Photochem. Photobiol., C* **2005**, *6*, 249−263.

(25) Frähmcke, J. S.; Walla, P. *J. Chem. Phys. Lett.* **2006**, *430*, 397−403.

(26) Czader, A.; Bittner, E. R. *J. Chem. Phys.* **2008**, *128*, No. 035101.

(27) Beljonne, D.; Curutchet, C.; Scholes, G. D.; Silbey, R. J. *J. Phys. Chem. B* **2009**, *113*, 6583−6599.

(28) Muñoz-Losa, A.; Curutchet, C.; Krueger, B. P.; Hartsell, L. R.; Mennucci, B. *Biophys. J.* **2009**, *96*, 4779−4788.

(29) Müh, F.; Madjet, M. E.-A.; Adolphs, J.; Abdurahman, A.; Rabenstein, B.; Ishikita, H.; Knapp, E.-W.; Renger, T. *Proc. Natl. Acad. Sci. U. S. A.* **2007**, *104*, 16862−16867.

(30) Adolphs, J.; Müh, F.; Madjet, M. E.-A.; Renger, T. *Photosynth. Res.* **2007**, *95*, 197−209.

(31) Raszewski, G.; Renger, T. *J. Am. Chem. Soc.* **2008**, *130*, 4431−4446.

(32) Olbrich, C.; Kleinekathöfer, U. *J. Phys. Chem. B* **2010**, *114*, 12427−12437.

(33) Olbrich, C.; Jansen, T. L. C.; Liebers, J.; Aghtar, M.; Strümpfer, J.; Schulten, K.; Knoester, J.; Kleinekathöfer, U. *J. Phys. Chem. B* **2011**, *115*, 8609−8621.

(34) Maj, M.; Jeon, J.; Góra, R. W.; Cho, M. *J. Phys. Chem. A* **2013**, *117*, 5909−5918.

(35) Aghtar, M.; Strümpfer, J.; Olbrich, C.; Schulten, K.; Kleinekathöfer, U. *J. Phys. Chem. Lett.* **2014**, *5*, 3131−3137.

(36) Sokalski, W.; Poirier, R. *Chem. Phys. Lett.* **1983**, *98*, 86−92.

(37) May, V.; Kühn, O. *Charge and Energy Transfer Dynamics in Molecular Systems*, 3rd ed.; Wiley-VCH Verlag: Weinheim, Germany, 2011; pp 467−543.

(38) Buckingham, A. D. *Q. Rev., Chem. Soc.* **1959**, *13*, 183−214.

(39) Stone, A. *The Theory of Intermolecular Forces*, 2nd ed.; University Press: Oxford, U.K., 2013; pp 122−140.

(40) Etchebest, C.; Lavery, R.; Pullman, A. *Theor. Chim. Acta* **1982**, *62*, 17−28.

(41) Stone, A. J. *J. Chem. Theory Comput.* **2005**, *1*, 1128−1132.

(42) Sigfridsson, E.; Ryde, U. *J. Comput. Chem.* **1998**, *19*, 377−395.

(43) Frisch, M. J.; Trucks, G. W.; Schlegel, H. B.; Scuseria, G. E.; Robb, M. A.; Cheeseman, J. R.; Scalmani, G.; Barone, V.; Mennucci, B.; Petersson, G. A.; Nakatsuji, H.; Caricato, M.; Li, X.; Hratchian, H. P.; Izmaylov, A. F.; Bloino, J.; Zheng, G.; Sonnenberg, J. L.; Hada, M.; Ehara, M.; Toyota, K.; Fukuda, R.; Hasegawa, J.; Ishida, M.; Nakajima, T.; Honda, Y.; Kitao, O.; Nakai, H.; Vreven, T.; Montgomery, J.; Peralta, J. E.; Ogliaro, F.; Bearpark, M.; Heyd, J. J.; Brothers, E.; Kudin, K. N.; Staroverov, V. N.; Kobayashi, R.; Normand, J.; Raghavachari, K.; Rendell, A.; Burant, J. C.; Iyengar, S. S.; Tomasi, J.; Cossi, M.; Rega, N.; Millam, J. M.; Klene, M.; Knox, J. E.; Cross, J. B.; Bakken, V.; Adamo, C.; Jaramillo, J.; Gomperts, R.; Stratmann, R. E.; Yazyev, O.; Austin, A. J.; Cammi, R.; Pomelli, C.; Ochterski, J. W.; Martin, R. L.; Morokuma, K.; Zakrzewski, V. G.; Voth, G. A.; Salvador, P.; Dannenberg, J. J.; Dapprich, S.; Daniels, A. D.; Farkas, O.; Foresman, J. B.; Ortiz, J. V.; Cioslowski, J.; Fox, D. J. *Gaussian 09*, Revision D.01; Gaussian: Wallingford, CT, USA, 2009.

(44) Shao, Y.; Molnar, L. F.; Jung, Y.; Kussmann, J.; Ochsenfeld, C.; Brown, S. T.; Gilbert, A. T. B.; Slipchenko, L. V.; Levchenko, S. V.; O'Neill, D. P.; DiStasio, R. A., Jr.; Lochan, R. C.; Wang, T.; Beran, G. J. O.; Besley, N. A.; Herbert, J. M.; Lin, C. Y.; Voorhis, T. V.; Chien, S.

H.; Sodt, A.; Steele, R. P.; Rassolov, V. A.; Maslen, P. E.; Korambath, P. P.; Adamson, R. D.; Austin, B.; Baker, J.; Byrd, E. F. C.; Dachsel, H.; Doerksen, R. J.; Dreuw, A.; Dunietz, B. D.; Dutoi, A. D.; Furlani, T. R.; Gwaltney, S. R.; Heyden, A.; Hirata, S.; Hsu, C.-P.; Kedziora, G.; Khalliulin, R. Z.; Klunzinger, P.; Lee, A. M.; Lee, M. S.; Liang, W.; Lotan, I.; Nair, N.; Peters, B.; Proynov, E. I.; Pieniazek, P. A.; Rhee, Y. M.; Ritchie, J.; Rosta, E.; Sherrill, C. D.; Simmonett, A. C.; Subotnik, J. E.; Woodcock, H. L., III; Zhang, W.; Bell, A. T.; Chakraborty, A. K.; Chipman, D. M.; Keil, F. J.; Warshel, A.; Hehre, W. J.; Schaefer, H. F., III; Kong, J.; Krylov, A. I.; Gill, P. M. W.; Head-Gordon, M. *Phys. Chem. Chem. Phys.* **2006**, *8*, 3172−3191.

(45) Fermann, J. T.; Valeev, E. F. *Libint: Machine-generated library for efficient evaluation of molecular integrals over Gaussians*, Version 1.1.4; 2003; http://libint.sourceforge.net/.

(46) Werner, H.-J.; Knowles, P. J.; Knizia, G.; Manby, F. R.; Schütz, M.; Celani, P.; Korona, T.; Lindh, R.; Mitrushenkov, A.; Rauhut, G.; Shamasundar, K. R.; Adler, T. B.; Amos, R. D.; Bernhardsson, A.; Berning, A.; Cooper, D. L.; Deegan, M. J. O.; Dobbyn, A. J.; Eckert, F.; Goll, E.; Hampel, C.; Hesselmann, A.; Hetzer, G.; Hrenar, T.; Jansen, G.; Köppl, C.; Liu, Y.; Lloyd, A. W.; Mata, R. A.; May, A. J.; McNicholas, S. J.; Meyer, W.; Mura, M. E.; Nicklass, A.; O'Neill, D. P.; Palmieri, P.; Peng, D.; Pflüger, K.; Pitzer, R.; Reiher, M.; Shiozaki, T.; Stoll, H.; Stone, A. J.; Tarroni, R.; Thorsteinsson, T.; Wang, M. *Molpro, a package of ab initio programs*, Version 2012.1; Molpro: Cardiff, U.K., 2012.

(47) Scholes, G. D.; Curutchet, C.; Mennucci, B.; Cammi, R.; Tomasi, J. *J. Phys. Chem. B* **2007**, *111*, 6978−6982.